## TECHNICAL NOTE

## **Magnetic Resonance in Medicine**

## In vivo <sup>1</sup>H MR spectroscopy with *J*-refocusing

Dinesh K. Deelchand<sup>1</sup> | Jamie D. Walls<sup>2</sup> | Małgorzata Marjańska<sup>1</sup>

## Correspondence

Dinesh K. Deelchand, Center for Magnetic Resonance Research, University of Minnesota, 2021 6th St SE, Minneapolis, MN 55455, USA. Email: deelc001@umn.edu

#### **Funding information**

National Institutes of Health, Grant/ Award Number: P30 NS076408 and P41 EB027061; National Science Foundation, Grant/Award Number: CHE-1807724 **Purpose:** The goal of this study was to propose a novel localized proton MR spectroscopy (MRS) sequence that reduces signal loss due to J-modulation in the rat brain in vivo. **Methods:** Sprague-Dawley rats were studied at 9.4 T. A semi-LASER sequence with evenly distributed echo-time ( $T_E$ ) was used, and a 90° J-refocusing pulse was inserted at  $T_E/2$ . Proton spectra were acquired at two  $T_E$ s (30 and 68 ms), with and without the J-refocused pulse. Data were processed in MATLAB and quantified with LCModel.

**Results:** The *J*-refocused spectrum acquired at  $T_E = 30$  ms did not show any signal losses due to *J*-modulation and had comparable spectral pattern to the one acquired with semi-LASER using the minimum achievable  $T_E$ . Higher signal amplitudes for glutamine,  $\gamma$ -aminobutyric acid and glutathione led to more reliable quantification precision for these metabolites. The refocused signal intensities at  $T_E = 68$  ms were also unaffected by *J*-modulation but were smaller than the signals at  $T_E = 30$  ms mainly due to transverse  $T_2$  relaxation of metabolites.

**Conclusion:** The proposed localized MRS sequence will be beneficial in both animal and human MRS studies when using ultra-short  $T_E$  is not possible while also providing more reliable quantification precision for *J*-coupled metabolites.

## KEYWORDS

9.4 T, brain, GABA, glutamine, glutathione, J-coupled metabolites, semi-LASER

## 1 | INTRODUCTION

Proton MR spectroscopy (MRS) enables non-invasive measurement of many metabolites in the brain. Certain metabolites, such as creatine and phosphocreatine, have only singlet resonances while other metabolites, such as N-acetylaspartate (NAA), phosphorylcholine (PCho), and glycerophosphorylcholine (GPC), consist of both singlet and multiplet peaks. In addition, a number of metabolites, such as glutamate (Glu), glutamine (Gln),  $\gamma$ -aminobutyric acid (GABA), and glutathione (GSH), have only J-coupled resonances. At ultra-short echo-times ( $T_E$ s), these J-coupled resonances are represented by in-phase multiplets that are relatively easy to quantify (based on their appropriate concentration levels) with prior

knowledge in the fit analysis. As  $T_E$  increases, however, these *J*-coupled metabolites undergo *J*-modulation, and their spectral patterns change as a function of  $T_E$ .<sup>3</sup> Based on the *J*-coupling constants and chemical shift differences between *J*-coupled partners, the spectral patterns might become completely dephased at a specific  $T_E$ , as in the case of Glu at 9.4 T and  $T_E = 45$  ms. In such instances, quantification of those metabolites might be difficult or impossible. To avoid these  $T_E$ -related issues, several studies<sup>4-6</sup> measuring  $T_2$  relaxation time constants of metabolites have used density-matrix simulations to determine the appropriate  $T_E$  values to use for quantifying either specific metabolites or the entire neurochemical profile.

To minimize *J*-modulation of the spectrum for coupled spin systems, the Carr-Purcell-Meiboom-Gill (CPMG) sequence,

© 2021 International Society for Magnetic Resonance in Medicine

<sup>&</sup>lt;sup>1</sup>Center for Magnetic Resonance Research, Department of Radiology, University of Minnesota, Minneapolis, Minnesota, USA

<sup>&</sup>lt;sup>2</sup>Department of Chemistry, University of Miami, Coral Gables, Florida, USA

which consists of multiple  $180^{\circ}$  pulses, is most commonly used. We have successfully shown that *J*-evolution can be reduced in the rat brain in vivo at 9.4 T using CP-LASER and  $T_{2\rho}$ -LASER sequences. However, owing to the multiple  $180^{\circ}$  pulses required for CPMG, this technique cannot be easily translated to human studies due to specific absorption rate (SAR) deposition issues at fields of 3 T and above.

Another interesting technique to suppress *J*-modulation, which was proposed in the late 1980s, is to apply a 90° pulse with an appropriate phase at the midpoint of a double spinecho sequence. This method seems promising for human studies due to the negligible SAR requirement of using only a single 90° pulse compared with the multiple 180° pulses required for conventional CPMG techniques. Several groups have shown the efficiency of suppressing *J*-modulation on phantom and tissue extracts using proton MRS, <sup>11-14</sup> and one group applied this technique in vivo with a focus on glutamate

detection using a complex pulse sequence that required four shots for 3D localization. <sup>15</sup> However, up to now, no study has successfully demonstrated this technique to work for a range of J-coupled metabolites that are present in the brain in vivo. Therefore, the aim of this study is to propose a novel sequence that enables the acquisition of localized proton MRS data with J-refocusing for coupled metabolites in the rat brain in vivo. The sequence, which is given in Figure 1A, is based on the semi-LASER<sup>16,17</sup> with an evenly distributed  $T_E$ .

## 2 | METHODS

## 2.1 | Localized *J*-refocused sequence

Several high-resolution NMR and phantom studies have previously demonstrated refocusing of *J*-modulation for weakly

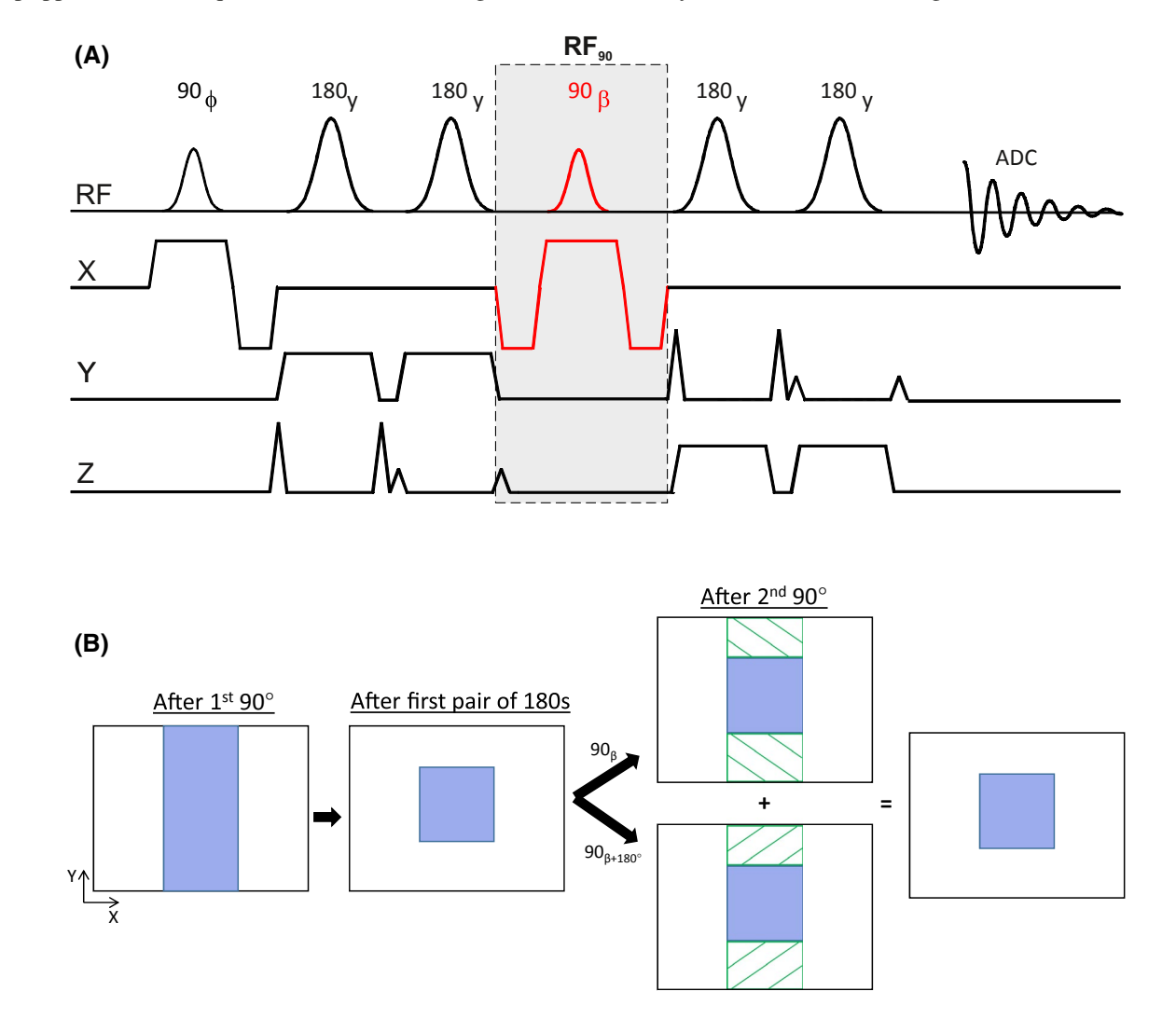


**FIGURE 1** A, Semi-LASER sequence with an additional slice-selective 90° pulse (RF<sub>90</sub> inside gray box) to suppress *J*-modulation of coupled metabolites. The phase of the RF<sub>90</sub> pulse is +90° relative to the first excitation pulse, e.g., if  $\phi = 0^\circ$  or 90° then  $\beta = 90^\circ$  or 180°, respectively. The sequence in A becomes a conventional semi-LASER by removing the RF<sub>90</sub> pulse and the dephasing rephasing gradients about the RF<sub>90</sub> pulse. B, Schematic depicting VOI selection in the transverse XY plane. After the first pair of adiabatic full passage (AFP) pulses, a bar selection (blue box) is achieved along Z-direction. However, applying the RF<sub>90</sub> pulse refocuses signal outside the VOI along the X-direction (green stripped box). The signals from a two-step phase cycle of the RF<sub>90</sub> phase, β and β+180°, are added to eliminate signal outside the VOI. ADC, analog-to-digital converter

and/or strongly coupled spin systems.  $^{9\cdot13}$  A double spin-echo sequence has been commonly used whereby a  $90^{\circ}$  pulse (denoted herein as  $RF_{90}$ ) is inserted at the time where the first echo occurs, i.e., at  $T_E/2$ , and the phase of the  $RF_{90}$  pulse was set to be  $+90^{\circ}$  relative to that of the first excitation pulse. In this work, the semi-LASER $^{16,17}$  was considered as the most suitable pulse sequence to incorporate the  $RF_{90}$  pulse, since it consists of an excitation pulse followed by two pairs of refocusing adiabatic full passage (AFP) pulses.

A 3D localized semi-LASER sequence was implemented by inserting a RF $_{90}$  pulse at time  $T_E/2$  (Figure 1A). The  $T_E$  was evenly distributed such that the inter-pulse delay between the AFP pulses was identical. The RF $_{90}$  was slice-selective and applied along the X-direction as was the first slice-selective excitation pulse. Dephasing and rephasing gradients were applied before and after the RF $_{90}$  pulse to make sure that the phase at the center of this pulse was zero for all spins in the selected slab. In this configuration, unwanted signal from outside the volume of interest (VOI) was refocused along the X-direction as shown in the schematic in Figure 1B. To eliminate such outside excitation, a simple two-step phase cycle on the RF $_{90}$  pulse was used such that the signals with RF $_{90}$  pulse phases of  $\beta$  and  $\beta$ +180° were added. Another option is to use a global non slice-selective RF $_{90}$  pulse. In this case,  $T_E$  would

were simulated with and without the refocusing  $RF_{90}$  pulse using the actual RF pulse durations (without gradients) and patterns as used for the in vivo studies described in the next section.

# 2.2 | Theoretical understanding of *J*-refocusing

While *J*-refocusing is perfect for a weakly coupled IS spin system,  $^9$  *J*-evolution in strongly and weakly coupled arbitrary spin systems can still be refocused to a high degree  $^{12}$  as long as  $\pi J_{max} \frac{T_E}{2} \ll 1$ , where  $J_{max}$  is the maximum spin-spin coupling within a molecule. To see this, consider the spin evolution in a weakly coupled spin system under the *J*-refocused sequence, which can be effectively described by a RF<sub>90Y</sub>–T<sub>E</sub>/2–RF<sub>90X</sub>–T<sub>E</sub>/2 pulse sequence where chemical shift evolution has been removed by the AFP pulse pairs leaving evolution under the spin-spin Hamiltonian in the weak-coupling limit,  $H = 2\pi \sum_{j < k} J_{jk} I_{Z,j} I_{Z,k}$ , during the T<sub>E</sub>/2 pe-

riods. In this case, the spin evolution under the J-refocused sequence can be described by the following set of transformations:

$$\sum_{j} I_{Z,j} \xrightarrow{90^{\circ}Y} \sum_{j} I_{X,j} \xrightarrow{\frac{T_{E}}{2}} \sum_{j} I_{X,j} f_{j} \left(\frac{T_{E}}{2}\right) + 2 \sum_{k \neq j} g_{jk} \left(\frac{T_{E}}{2}\right) I_{Y,j} I_{Z,k}$$

$$+ O\left[\left(\frac{\pi J T_{E}}{2}\right)^{2}\right] \xrightarrow{90^{\circ}X} \sum_{j} I_{X,j} f_{j} \left(\frac{T_{E}}{2}\right) - 2 \sum_{k \neq j} g_{kj} \left(\frac{T_{E}}{2}\right) I_{Y,j} I_{Z,k}$$

$$+ O\left[\left(\frac{\pi J T_{E}}{2}\right)^{2}\right] \xrightarrow{\frac{T_{E}}{2}} \sum_{j} I_{X,j} \left(\left(f_{j} \left(\frac{T_{E}}{2}\right)\right)^{2} + \sum_{k \neq j} g_{kj} \left(\frac{T_{E}}{2}\right) g_{jk} \left(\frac{T_{E}}{2}\right)\right)$$

$$+ 2 \sum_{k \neq j} I_{Y,j} I_{Z,k} f_{j} \left(\frac{T_{E}}{2}\right) \left(g_{jk} \left(\frac{T_{E}}{2}\right) - g_{kj} \left(\frac{T_{E}}{2}\right)\right)$$

$$+ O\left[\left(\frac{\pi J T_{E}}{2}\right)^{2}\right] \equiv \sum_{j} Signal_{j,in-phase}^{Refocused} \left(T_{E}\right) I_{X,j} + 2 \sum_{k \neq j} Signal_{jk,anti-phase}^{Refocused} \left(T_{E}\right) I_{Y,j} I_{Z,k} + O\left[\left(\frac{\pi J T_{E}}{2}\right)^{2}\right]$$

be further shortened on the order of 0.5 to 1 ms on animal scanners and approximately 2 to 3 ms on human scanners by no longer requiring dephasing/rephrasing gradients about the  $RF_{90}$ . In this configuration, more signals would be introduced outside the VOI in both the X and Y directions compared to only Y direction when a slice-selective  $RF_{90}$  was used. While a two-step phase cycling would still be necessary to remove the signal outside the VOI, cycling out these higher outside signals would generally be more susceptible to subtraction artifacts, especially in human studies.

The change in spectral pattern as  $T_E$  increased from  $T_E$  = 20 to  $T_E$  = 100 ms was investigated using density matrix simulations<sup>19</sup> for several strongly and weakly coupled metabolites such as Gln, GABA, GSH, and lactate (Lac). Spectra

where  $O\left[\left(\frac{\pi J T_{\rm E}}{2}\right)^2\right]$  in Equation (1) denotes three-spin or higher coherences,  $f_j\left(\tau\right) = \prod_{j \neq k} \cos\left(\pi J_{jk}\tau\right)$ ,  $g_{jk}\left(\tau\right) = \sin\left(\pi J_{jk}\tau\right) \prod_{m \neq j,k} \cos\left(\pi J_{jm}\tau\right)$ , and  $Signal_{j,in-phase}^{Refocused}\left(T_E\right)$  and  $Signal_{jk,anti-phase}^{Refocused}\left(T_E\right)$  are the in-phase and anti-phase contributions to the signal at  $T_{\rm E}$  from the  $j^{th}$  spin, respectively. For comparison, the corresponding in-phase and anti-phase contributions to the signal at  $T_{\rm E}$  from the  $j^{th}$  spin without the refocusing  $RF_{90}$  are  $Signal_{j,in-phase}^{Unrefocused}\left(T_E\right) = f_j\left(T_E\right)$  and  $Signal_{jk,anti-phase}^{Unrefocused}\left(T_E\right) = g_{jk}\left(T_E\right)$ , respectively.

In Equation (1), *J*-evolution is effectively refocused when  $J_{jk}T_E \leq \frac{1}{3}$  for all spins j and k within a molecule since to first-order in  $J_{jk}T_E$ ,  $f_j\left(\frac{T_E}{2}\right) \approx 1$ ,  $g_{jk}\left(\frac{T_E}{2}\right) \approx \frac{\pi J_{jk}T_E}{2}$ , and thus

## -Magnetic Resonance in Medicine-

 $\begin{aligned} &\textit{Signal}_{j,in-phase}^{\textit{Refocused}}\left(T_{E}\right) \approx 1 \quad \text{and} \quad &\textit{Signal}_{jk,anti-phase}^{\textit{Refocused}}\left(T_{E}\right) \approx 0. \\ &\text{Note that even for } J_{max}T_{E} \leq \frac{1}{2}, \, &\textit{Signal}_{jk,anti-phase}^{\textit{Refocused}}\left(T_{E}\right) \text{ is still} \\ &\text{smaller than } &\textit{Signal}_{jk,anti-phase}^{\textit{Unrefocused}}\left(T_{E}\right) \text{:} \end{aligned}$ 

$$\begin{aligned} Signal_{jk,anti-phase}^{Refocused} \left( T_E \right) &= \\ &\left| \frac{\sin \left( \pi J_{jk} T_E \right)}{2} \left( \prod_{m \neq j,k} \cos^2 \left( \frac{\pi J_{jm} T_E}{2} \right) - \prod_{m \neq j,k} \cos \left( \frac{\pi J_{jm} T_E}{2} \right) \cos \left( \frac{\pi J_{km} T_E}{2} \right) \right) \right| \\ &\leq \left| \sin \left( \pi J_{jk} T_E \right) \prod_{m \neq j,k} \cos \left( \pi J_{jk} T_E \right) \right| \end{aligned}$$

$$(2)$$

## 2.3 | In vivo measurements

Male Sprague-Dawley rats (n = 3) were studied using a horizontal-bore 9.4-T scanner (Magnex Scientific, Oxford, UK) interfaced to an Agilent DirectDrive console (Agilent Technologies, CA). Animals were anesthetized with 1.5% isoflurane in a mixture of 50% O<sub>2</sub>:50% N<sub>2</sub>O and placed in a cradle with the head fixed using a bite-bar and ear rods. Throughout the study, the animals' body temperature was monitored and maintained at 37°C using hot water circulation. All studies were approved by the Institutional Animal Care and Use Committee at the University of Minnesota.

In semi-LASER, a 1.0 ms Shinnar–Le Roux pulse (bandwidth = 13 kHz) was used for both excitation and for the RF $_{90}$  pulse, and 1.5 ms AFP pulses (HS1, bandwidth = 16.7 kHz) were used for refocusing. Water suppression (bandwidth = 270 Hz) was achieved using the VAPOR technique with interleaved outer-volume suppression pulses. A home-built quadrature surface radiofrequency coil (two loops, 14 mm diameter each) was used as a transceiver.

MRS data were acquired from a 180 µL VOI in the rat brain. At the start of the experiment, fast spin-echo images were acquired and used to position the VOI within tissue containing the hippocampus, thalamus and the midbrain. B<sub>0</sub> inhomogeneity in the selected VOI was adjusted using an adiabatic version of FASTESTMAP technique.<sup>21</sup> The mean measured water linewidth using the real component was 18 Hz. Semi-LASER water-suppressed spectra (repetition time of 4 s, spectral width of 10 kHz) at  $T_E = 30$  ms (32 averages) and  $T_E = 68$  ms (128 averages) were acquired in an interleaved fashion switching between enabling and disabling the RF<sub>90</sub> pulse. Water reference scans were also acquired for quantification and for eddy-current correction. A T<sub>E</sub> of 30 ms was considered since this is the shortest T<sub>E</sub> typically achieved on the human clinical scanner at 3 T while a T<sub>E</sub> of 68 ms was chosen to see the viability of using this J-refocused sequence for editing.

All MRS spectra were processed in MATLAB using MRspa software.  $^{22}$  The data with and without RF $_{90}$  were

post-processed as two separate measurements. Frequency and phase corrections were performed followed by eddy current correction.<sup>23</sup> The resulting summed semi-LASER spectra (with and without an RF<sub>90</sub> pulse) were fitted using LCModel v6.3-0G.<sup>24</sup> Two basis sets, each consisting of 18 simulated spectra, were used as previously described<sup>8</sup> together with the built-in macromolecular resonances in LCModel.

## 3 | RESULTS

Simulations of the total signal integral (with and without the refocusing RF<sub>90</sub> pulse) as a function of  $T_E$  for Gln, GABA, GSH, and Lac are shown in Figure 2. Even at the shortest  $T_E = 20$  ms at 9.4 T, these metabolites underwent some *J*-modulation when the RF<sub>90</sub> pulse was not applied. Interestingly, more than 15% of the total signals were recovered with the refocusing pulse. As  $T_E$  increased, the signal integral decreased even though the spectral pattern was always positive. Compared to the other *J*-coupled metabolites in Figure 2, lactate, which is a weakly coupled spin system, exhibited relatively smaller *J*-modulation and changes in signal amplitude with and without an RF<sub>90</sub> pulse.

The effect of the refocusing  $RF_{90}$  pulse on the spectral pattern at  $T_E=30$  ms is shown in Figure 2. As expected, the simulated spectrum with  $RF_{90}$  pulse was much higher in intensity compared to the normal semi-LASER spectrum at the same  $T_E$ . For instance, the signal intensities for all resonances of Gln, GABA and Lac were at least twice as large with an  $RF_{90}$  pulse compared to the case without an  $RF_{90}$  pulse. Interestingly, the signal intensities from the cysteine and glutamate moieties in GSH, which are strongly coupled systems, were larger with an  $RF_{90}$  pulse compared to the signal intensities in a glycine moiety, which is a weakly coupled system.

In vivo spectra acquired from a rat brain are shown in Figure 3. Visible differences in signal intensities were observed between spectra acquired with and without an RF<sub>90</sub> pulse, especially for Glu, Gln, GABA, and a multiplet of NAA (mNAA), which were consistent with the simulations in Figure 2. The effects of the RF<sub>90</sub> pulse were especially significant at longer T<sub>E</sub> where larger *J*-modulation would be expected if not for application of the *J*-refocusing pulse. Moreover, *J*-modulation of the macromolecular resonances, particularly those at 0.89 and 1.70 ppm that are from *J*-coupled systems, <sup>26</sup> was refocused at both T<sub>E</sub>s by application of an RF<sub>90</sub> pulse. Last, the intensity of the singlets of NAA, total creatine (tCr), and total choline (tCho) were unaffected by the *J*-refocusing pulse as expected. The signal-to-noise ratios (SNR) for tNAA peak measured for this animal were 99

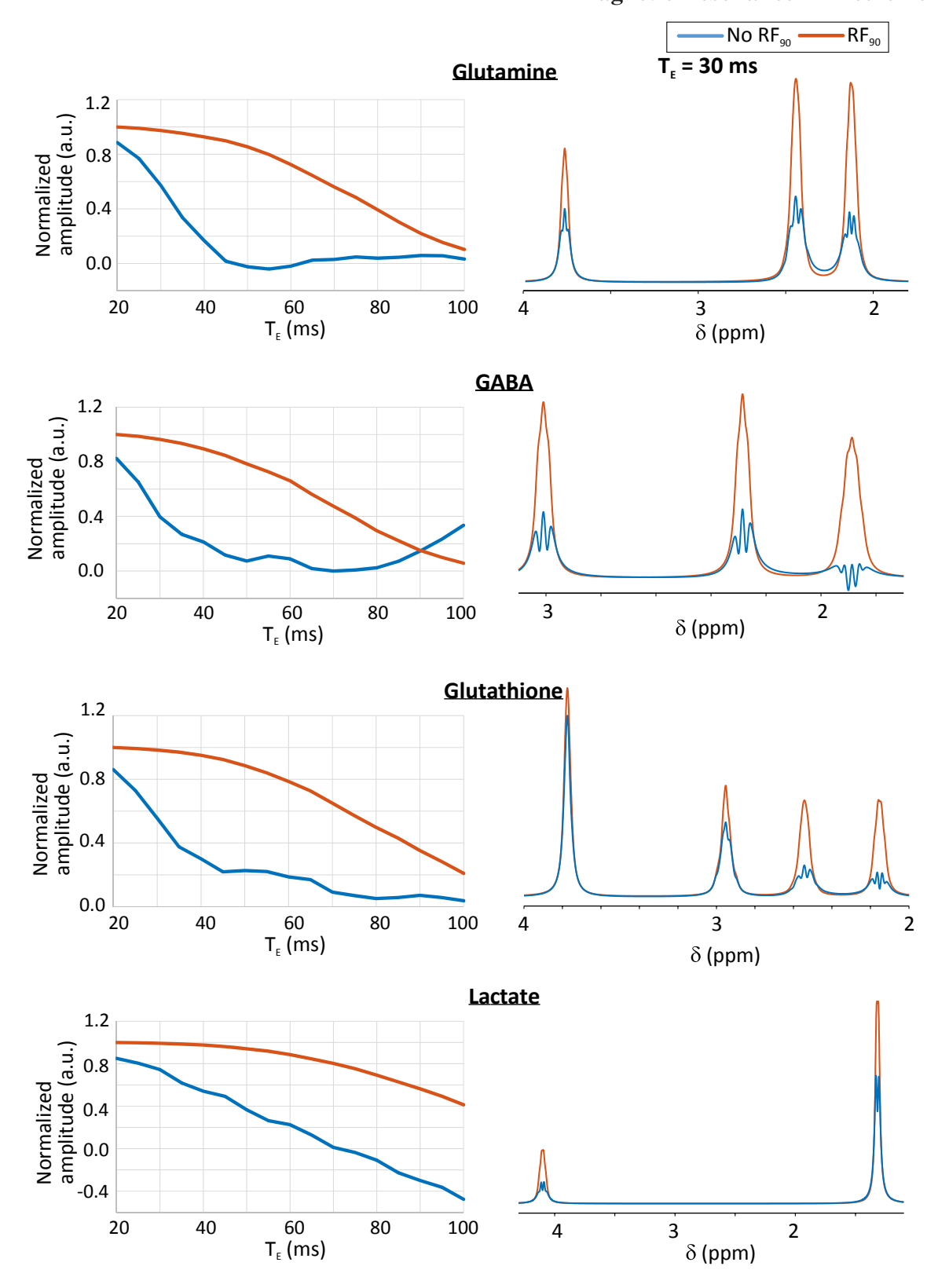


**FIGURE 2** Left column, *J*-refocusing of Gln, GABA, GSH and Lac using semi-LASER at 9.4 T; standard semi-LASER (blue curve) and semi-LASER with an additional RF<sub>90</sub> pulse (red curve). Signal integrals correspond to the amplitude of the first point of the simulated FID normalized to 1.0 at  $T_E = 20$  ms when the RF<sub>90</sub> pulse was enabled.  $T_2$  relaxation and gradients were neglected in the simulation. Right column, Simulated spectra without (blue) and with (red) the RF<sub>90</sub> pulse are shown at  $T_E = 30$  ms. All spectra were line-broadened by 10 Hz for display purposes

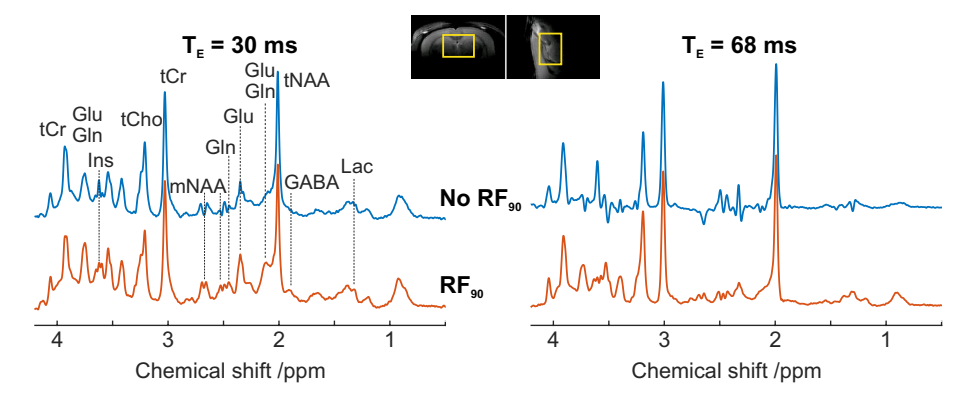


**FIGURE 3** In vivo semi-LASER spectra acquired with (red) and without (blue) a J-refocusing RF $_{90}$  pulse from one animal at  $T_E = 30$  ms (left) and  $T_E = 68$  ms (right). When an RF $_{90}$  pulse was applied, the signal intensities from all J-coupled metabolites were higher compared to the case without an RF $_{90}$  pulse. The macromolecular spectrum at both  $T_E$ s also changed with the inclusion of an RF $_{90}$  pulse. All spectra were line broadened with a 1.5 Hz Gaussian line broadening for display purposes only. Insert shows the VOI location on axial and sagittal turbo spin-echo images. The dotted vertical lines are visual guides pointing to J-coupled metabolites in which J-refocusing is easily observed in the spectra

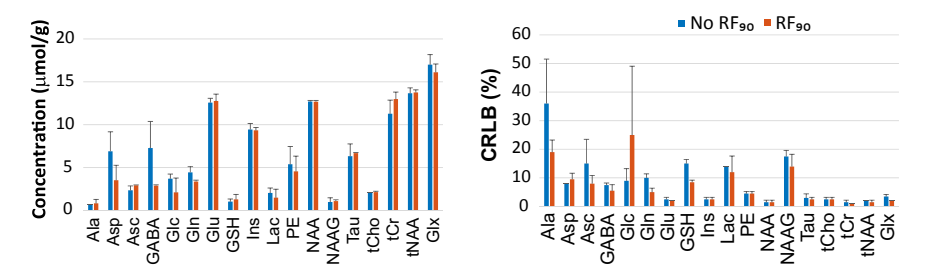


**FIGURE 4** Neurochemical concentrations (left) and the corresponding CRLB (right) measured at  $T_E = 30$  ms using the semi-LASER sequence with (red) and without (blue) an RF<sub>90</sub> pulse. Error bars represent SDs between n = 3 animals. Ins, *myo*-inositol; PE, phosphoethanolamine; NAAG, *N*-acetyl-aspartyl-glutamate; Tau, taurine; tNAA, NAA+NAAG; Glx, glutamate+glutamine

vs. 96 at  $T_E = 30$  ms and 152 vs. 146 at  $T_E = 68$  ms without and with the RF<sub>90</sub> pulse, respectively.

For  $T_E = 30$  ms, the spectra with an RF<sub>90</sub> pulse for Jcoupled metabolites did not seem to undergo any significant J-modulation and were similar to the spectra acquired at the minimum achievable T<sub>E</sub> of 19 ms (data not shown). However, the concentrations of almost all measured metabolites at T<sub>E</sub> = 30 ms determined from the MR spectra with and without an RF<sub>90</sub> pulse were similar as shown in Figure 4, with the exceptions of aspartate (Asp) and GABA. As a result of Jmodulation, these metabolites were overestimated due to their out-of-phase J-modulated spectral pattern when no RF<sub>90</sub> was applied, whereas the refocusing the *J*-modulation led to an in-phase spectral pattern that provided better quantification. Interestingly, a gain in quantification precision as reflected by the lower Cramer-Rao lower bound (CRLB) values was observed for alanine (Ala), ascorbate (Asc), GABA, Gln, GSH, and Lac as shown in Figure 4. Glucose (Glc) was the only metabolite where the CRLB was found to increase when using the *J*-refocused pulse.

At  $T_E = 68$  ms, as the *J*-coupled metabolites underwent further *J*-modulation in addition to  $T_2$  relaxation, the refocused signal intensities were lower compared to those

acquired at  $T_E = 30$  ms with  $RF_{90}$  pulse as shown in Figure 3. For instance, the Gln signal integral was almost null at this  $T_E$  without an  $RF_{90}$  pulse but was almost 60% higher with an  $RF_{90}$  (Figure 3). However, the CRLB at  $T_E = 68$  ms was comparable with and without the *J*-refocusing pulse (data not shown). This was most likely due to the distinct spectral patterns for Glu, Gln, and mNAA that were observed even without an  $RF_{90}$  pulse. Due to the small number of animals studied (n = 3), no statistical analysis was carried out.

Application of two slice-selective 90° pulses along the X-direction resulted in smoothed edges in the VOI profile along the X-direction as shown in Figure 5. Consequently, the VOI profiles in Y and Z direction were also lowered. Application of a *J*-refocusing pulse resulted in ~10% loss of water reference signal measured in vivo.

## 4 DISCUSSION

The current study demonstrates that *J*-evolution of coupled metabolites can be refocused by inserting a 90° pulse with appropriate phase into the semi-LASER sequence. Since the majority of *J*-couplings for the metabolites studied in this

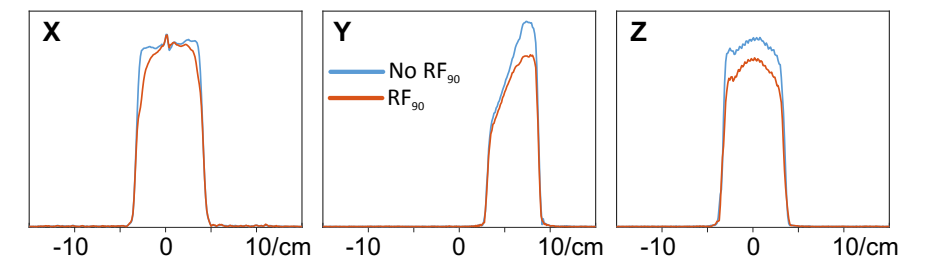


**FIGURE 5** VOI profiles measured along the X, Y, and Z directions from a rat brain in vivo using the semi-LASER sequence ( $T_E = 19$  ms, field of view = 3 cm, 256 complex points, spectral width = 100 kHz). Plots show the effect of an RF<sub>90</sub> pulse on the VOI profiles (red curves with the RF<sub>90</sub> pulse, and blue curves without the RF<sub>90</sub> pulse). The profile along X-direction was smoothed on the edges due to applying two slice-selective 90° pulses

work ranged between 6 and 8 Hz, J-evolution was refocused using the *J*-refocused sequence at  $T_E = 30$  ms since  $\frac{\pi J T_E}{2} < \frac{\pi}{6}$ . Since  $0.64 \le \frac{\pi J T_E}{2} \le 0.86$  for  $T_E = 68$  ms, however, some signal attenuation and J-modulation occurred although the RF<sub>90</sub> pulse still reduced the overall amount of J-modulation since  $JT_E \cong \frac{1}{4}$ . With the proposed *J*-refocused sequence, a perfect spin-echo signal was measured at full signal intensity due to sandwiching the second RF<sub>90</sub> between dephasing/rephasing gradients which resulted in an RF pulse with uniform phase applied throughout the sample. This is in contrast to a previous study<sup>11</sup> where 50% of the signal was lost (either dephased or placed along z-direction) due to sandwiching the second RF<sub>90</sub> between spoiler gradients. The higher signal amplitudes due to suppressing J-modulation with an RF<sub>90</sub> pulse imply higher SNR for Gln, GABA, and GSH, and this in turn leads to more reliable quantification precision of these metabolites. Although the novel sequence requires a two-step phase cycle to achieve good localization, the spectral patterns measured at relatively short  $T_E = 30$  ms were comparable and only slightly lower in intensity due to T2 relaxation to the spectrum acquired using the shortest achievable T<sub>E</sub>.

One potential benefit of utilizing this novel sequence is for MRS studies where ultra-short T<sub>E</sub> cannot be realized. For example, surface RF coils are typically used to achieve high transmit B<sub>1</sub> fields and SNR<sup>27,28</sup> during MRS studies in animals. However, this only allows for investigating brain regions close to the surface and is dependent on the size of the surface coil. For deeper brain regions such as in the hypothalamus or pons in rodents, a volume RF coil, which has less B<sub>1</sub> efficiency than a surface coil, is generally required. Due to the poorer B<sub>1</sub> transmit efficiency of volume RF coils, longer pulse durations are required thereby increasing the minimum achievable T<sub>E</sub> to times that are greater than 30 ms for pulse sequences such as semi-LASER or LASER.<sup>29</sup> A weak gradient coil might also prolong the minimum T<sub>E</sub> since longer spoiler gradient durations would also be required to obtain good localization. In either case, the proposed MRS sequence would be useful since the spectral patterns under J-refocusing and measured at the minimal T<sub>E</sub> with a volume coil would be comparable to the spectral patterns measured at ultra-short  $T_{\rm E}$  using a surface coil and will provide similar quantification accuracy.

Another potential advantage of using the *J*-refocused sequence is the increase in quantification precision of J-coupled metabolites at 3 T (e.g., Glu+Gln, GSH, myo-inositol) and 7 T (e.g., Gln, Glu, GSH, myo-inositol, taurine) in human studies when using relatively long T<sub>E</sub>s of 25 to 40 ms. On clinical 3 T and 7 T MR scanners, volume coils (e.g., standard body coil or transverse electromagnetic [TEM] coil) are typically used whereby the minimal achievable T<sub>E</sub> is around 30 ms with a semi-LASER sequence. With the additional RF90 pulse and dephase/rephasing gradients, this T<sub>E</sub> would increase to about 35 ms. As mentioned above, the spectrum measured at this  $T_{\rm F}$ would be comparable to ultra-short T<sub>E</sub> data, thereby allowing for better quantification of coupled metabolites.<sup>30</sup> Although a gain in CRLB for J-coupled metabolites is expected when using this *J*-refocused sequence in human studies, the values are hard to predict based on animal data. This is because, in animals, the spectral linewidths are narrower and the T<sub>2</sub> relaxation times are longer compared to humans at a given field strength.<sup>31</sup> The expected gain in CRLB also depends on several factors, such as bandwidth of RF pulses, inter-pulse delay, VOI dimension, number of averages used and the B<sub>0</sub> field strength used in the study.

While the current study used a semi-LASER sequence, the *J*-refocusing pulse can be easily inserted into other localized proton MRS sequences that contain refocusing pulses, such as PRESS<sup>32</sup> and SPECIAL. <sup>33</sup> *J*-refocused PRESS might be a good alternative on animal scanners but is not recommended for human studies due to the larger chemical shift displacement error arising from the low bandwidth of the refocusing pulses. <sup>34</sup> For *J*-refocused SPECIAL, which uses two non-adiabatic 180° pulses, the phase cycle would have to be doubled to four scans to obtain 3D localization. <sup>33</sup> Note also that an RF<sub>90</sub> pulse cannot be inserted between a pair of AFP pulses, such as those used in semi-adiabatic SPECIAL, <sup>34</sup> due to the quadratic phase generated under AFP pulses.

One downside of the proposed sequence is that the voxel shape is affected from the application of two gradient-selective 90° pulses. The selected 3D VOI is not cuboidal in

## Magnetic Resonance in Medicine

shape anymore but rather a cuboid with a smoothed edge in the direction where the  $RF_{90}$  pulse is applied. As discussed earlier, sharper voxel shapes could be obtained using a single gradient-selective excitation pulse and a global  $RF_{90}$  pulse for J-refocusing, although such modifications are more prone to subtraction artifacts outside the VOI. Even though inclusion of an  $RF_{90}$  pulse led to a 10% loss in water signal, the gain in intensity for J-coupled metabolites outweighs the loss in VOI selection. Since both water reference and metabolite signals are acquired from the same VOI with the refocusing pulse, this should not affect metabolite quantification as demonstrated by the data in Figure 4.

## 5 | CONCLUSIONS

In summary, this study demonstrates the feasibility of acquiring  $^1H$  MRS data with reduced J-modulation over a wide range of  $T_E$ . The proposed localized MRS sequence will be beneficial in both animal and human MRS studies when ultra-short  $T_E$  is not possible and will provide more reliable quantification precision for J-coupled metabolites. Future work includes assessing the proposed sequence in the human brain.

## **ACKNOWLEDGMENTS**

The authors thank Lynn Utecht for expert technical assistance. J.D.W. acknowledges support from the National Science Foundation under grant CHE-1807724. This work was supported by NIH grants P41 EB027061 and P30 NS076408.

## **ORCID**

Dinesh K. Deelchand https://orcid. org/0000-0003-4266-4780 Małgorzata Marjańska https://orcid. org/0000-0002-4727-2447

## REFERENCES

- Pfeuffer J, Tkac I, Provencher SW, Gruetter R. Toward an in vivo neurochemical profile: quantification of 18 metabolites in short-echo-time <sup>1</sup>H NMR spectra of the rat brain. *J Magn Reson*. 1999;141:104-120.
- de Graaf RA. In Vivo NMR Spectroscopy. Hoboken, NJ: John Wiley & Sons Ltd; 2007.
- Deelchand DK, Henry P-G, Ugurbil K, Marjanska M. Measurement of transverse relaxation times of J-coupled metabolites in the human visual cortex at 4 T. Magn Reson Med. 2012;67: 891-897.
- Deelchand DK, Auerbach EJ, Kobayashi N, Marjańska M. Transverse relaxation time constants of the five major metabolites in human brain measured in vivo using LASER and PRESS at 3 T. Magn Reson Med. 2018;79:1260-1265.
- Deelchand DK, Auerbach EJ, Marjańska M. Apparent diffusion coefficients of the five major metabolites measured in the human brain in vivo at 3T. Magn Reson Med. 2018;79:2896-2901.

- Ganji SK, Banerjee A, Patel AM, et al. T2 measurement of J-coupled metabolites in the human brain at 3T. NMR Biomed. 2012;25:523-529.
- Allerhand A. Analysis of Carr-Purcell spin-echo NMR experiments on multiple-spin systems. I. The effect of homonuclear coupling. *J Chem Phys.* 1966;44:1-9.
- Deelchand DK, Henry P-G, Marjańska M. Effect of Carr-Purcell refocusing pulse trains on transverse relaxation times of metabolites in rat brain at 9.4 Tesla. *Magn Reson Med.* 2015;73:13-20.
- van Zijl PCM, Moonen CTW, von Kienlin M. Homonuclear J refocusing in echo spectroscopy. J Magn Reson. 1990;89:28-40.
- Takegoshi K, Ogura K, Hikichi K. A perfect spin echo in a weakly homonuclear J-coupled two spin-1/2 system. *J Magn Reson*. 1989;84:611-615.
- Lin Y, Lin L, Wei Z, Zhong J, Chen Z. Localized one-dimensional single voxel magnetic resonance spectroscopy without J coupling modulations. *Magn Reson Med*. 2016;76:1661-1667.
- Aguilar JA, Nilsson M, Bodenhausen G, Morris GA. Spin echo NMR spectra without J modulation. *Chem Commun*. 2012:48:811-813.
- Lee HK, Yaman A, Nalcioglu O. Homonuclear J-refocused spectral editing technique for quantification of glutamine and glutamate by 1H NMR spectroscopy. *Magn Reson Med.* 1995;34:253-259.
- Ronen I, O'Reilly T, Froeling M, Webb AG. Proton nuclear magnetic resonance J-spectroscopy of phantoms containing brain metabolites on a portable 0.05 T MRI scanner. *J Magn Reson*. 2020;320:106834.
- Pan JW, Mason GF, Pohost GM, Hetherington HP. Spectroscopic imaging of human brain glutamate by water-suppressed J-refocused coherence transfer at 4.1 T. Magn Reson Med. 1996;36:7-12.
- Scheenen TWJ, Klomp DWJ, Wijnen JP, Heerschap A. Short echo time 1H-MRSI of the human brain at 3T with minimal chemical shift displacement errors using adiabatic refocusing pulses. *Magn Reson Med.* 2008;59:1-6.
- 17. Öz G, Tkac I. Short-echo, single-shot, full-intensity proton magnetic resonance spectroscopy for neurochemical profiling at 4 T: validation in the cerebellum and brainstem. *Magn Reson Med*. 2011;65:901-910.
- Warren WS. Effects of arbitrary laser or NMR pulse shapes on population inversion and coherence. J Chem Phys. 1984;81:5437-5448.
- Henry PG, Marjańska M, Walls JD, Valette J, Gruetter R, Ugurbil K. Proton-observed carbon-edited NMR spectroscopy in strongly coupled second-order spin systems. *Magn Reson Med*. 2006;55:250-257.
- Tkac I, Starcuk Z, Choi IY, Gruetter R. In vivo 1H NMR spectroscopy of rat brain at 1 ms echo time. Magn Reson Med. 1999;41:649-656.
- 21. Gruetter R, Tkac I. Field mapping without reference scan using asymmetric echo-planar techniques. *Magn Reson Med*. 2000;43:319-323.
- Deelchand DK. MRspa: Magnetic Resonance Signal Processing and Analysis. https://www.cmrr.umn.edu/downloads/mrspa/ Aug 2018.
- Klose U. In vivo proton spectroscopy in presence of eddy currents. Magn Reson Med. 1990;14:26-30.
- Provencher SW. Estimation of metabolite concentrations from localized in vivo proton NMR spectra. Magn Reson Med. 1993;30:672-679.
- 25. Govind V. 1H-NMR chemical shifts and coupling constants for brain metabolites. *eMagRes*. 2016;5:1347-1362.
- Cudalbu C, Behar KL, Bhattacharyya PK, et al. Contribution of macromolecules to brain 1H MR spectra: experts' consensus recommendations. NMR Biomed. 2020;34:e4393.

- Vaughan JT, Adriany G, Garwood M, et al. Detunable transverse electromagnetic (TEM) volume coil for high-field NMR. *Magn Reson Med*. 2002;47:990-1000.
- 28. Pfeuffer J, Tkac I, Choi IY, et al. Localized in vivo 1H NMR detection of neurotransmitter labeling in rat brain during infusion of [1-13C] D-glucose. *Magn Reson Med*. 1999;41:1077-1083.
- Garwood M, DelaBarre L. The return of the frequency sweep: designing adiabatic pulses for contemporary NMR. *J Magn Reson*. 2001;153:155-177.
- Mekle R, Mlynárik V, Gambarota G, Hergt M, Krueger G, Gruetter R. MR spectroscopy of the human brain with enhanced signal intensity at ultrashort echo times on a clinical platform at 3T and 7T. *Magn Reson Med.* 2009;61:1279-1285.
- 31. Deelchand DK, Moortele P-F, Adriany G, et al. In vivo <sup>1</sup>H NMR spectroscopy of the human brain at 9.4 T: initial results. *J Magn Reson*. 2010;206:74-80.

- 32. Bottomley PA. Spatial localization in NMR spectroscopy in vivo. Ann NY Acad Sci. 1987;508:333-348.
- Mlynárik V, Gambarota G, Frenkel H, Gruetter R. Localized shortecho-time proton MR spectroscopy with full signal-intensity acquisition. *Magn Reson Med*. 2006;56:965-970.
- Öz G, Deelchand DK, Wijnen JP, et al. Working group on advanced single voxel HM. Advanced single voxel 1H magnetic resonance spectroscopy techniques in humans: experts' consensus recommendations. NMR Biomed. 2020;34:e4236.

**How to cite this article:** Deelchand DK, Walls JD, Marjańska M. In vivo <sup>1</sup>H MR spectroscopy with *J*-refocusing. *Magn Reson Med*. 2021;86:2957–2965. https://doi.org/10.1002/mrm.28936